Spectroscopic study of vacuum arc plasma expansion

Zhipeng Zhou[1,2], Andreas Kyritsakis[2], Zhenxing Wang[1*], Yi Li[1], Yingsan Geng[1], Flyura Djurabekova[2,3]

[1] *State Key Laboratory of Electrical Insulation and Power Equipment, Xi'an Jiaotong University, Xi'an 710049, China*

[2] *Helsinki Institute of Physics and Department of Physics, University of Helsinki, P.O. Box 43, FI-00014 Helsinki, Finland*

[3] *National Research Nuclear University MEPhI, Kashirskoye sh. 31, 115409 Moscow, Russia*

*zxwang@xjtu.edu.cn

Abstract

Vacuum breakdown (also known as arc or discharge) occurs when a sufficiently high electric field is applied between two electrodes in vacuum. The discharge is driven by the formation of an intensively glowing plasma at the cathode, which is followed by the ignition of an anode flare that gradually expands and fills the gap. Although it has been shown that the anode electrode does not play a significant role in the breakdown initiation, the nature of the anodic glow is of paramount importance for understanding the breakdown evolution. In this work, we use time- and space-resolved spectroscopy to study the anode flare. By using different anode and cathode materials, we find that excitations from both anode and cathode ions and neutrals contribute to the anodic glow. This implies that the cathodic plasma expands towards the anode without emitting any detectable light and starts glowing only when it reaches and interacts with the anode electrode. This interaction causes the introduction of anodic species in the plasma. The latter starts producing an expanding glow which contains spectra from both the cathode and anode materials and gradually fills the gap as the plasma equilibrates. Finally, we observe that after a breakdown, cathode material deposits on the anode electrode, gradually coating it. After hundreds of breakdowns, this coating covers the anode, resulting in the decay and possible elimination of the anode material signal in the spectra.

1. Introduction

With the widespread use of electrical energy in industry and in everyday life, electrical discharges become a very common phenomenon. As long as the potential gradient is high enough, a discharge can occur in any environment, including solids, liquids, gases, and even vacuum[1-4]. Electrical discharges in vacuum, also called vacuum breakdowns, are sustained by the erosion of metal electrodes. This kind of discharge can be found in fusion devices[5, 6], satellite systems[7, 8] and vacuum interrupters[1], which may face high electric field, and affects their reliability. In ultra-high electric field applications like the Compact Linear Collider (CLIC)[9-11] and micro or nano electromechanical system (MEMS or NEMS) and capacitors[12, 13], where the field reaches hundreds of MV/m, the occurrence of vacuum breakdown is even more harmful. For instance, microfabricated devices, such as the nano electrospray thruster arrays for spacecraft, may withstand large electric fields between electrodes, but if proper care is not taken, discharges can occur, destroying the whole chip[14]. Also, the high accelerating field of 10^8 V/m in CLIC causes vacuum arcs near the surfaces of the

accelerating structures, resulting in beam destabilization, surface degradation and structural damage of the accelerator[10].

The stable stage of a vacuum breakdown characterized by low burning voltage and high current conduction is often called vacuum arc, although this term is also commonly used to describe the whole breakdown process. Since we are here studying the very evolution of the breakdown, we shall use the former definition of the term. In the very beginning of a vacuum discharge, the voltage between the cathode and anode is still very high, while the gap current is relatively low. As the breakdown process evolves, the current gradually rises at the same time when the voltage drops, until a transition to the stable vacuum arc stage is finished. This paper focuses on the transient phenomena before the transition to the stable vacuum arc stage.

The evolution process of a vacuum breakdown involves activities on both the cathode and the anode electrodes. The majority of both theoretical and experimental studies suggested that a vacuum breakdown is initiated on the cathode surface, where many microscopic protrusions enhance the local electric field to a critical value. Mesyats et al. [15, 16] have proposed the ECTON model in which strong explosive electron emission is triggered on the cathode surface when micro tips are overheated by the electron emission currents. Simulations by using the Particle-In-Cell (PIC) method show that a vacuum breakdown can be initiated on the cathode if the evaporation rate of atoms from it is sufficient [17, 18]. In a recent work [19], multi-scale atomistic simulations revealed a thermal runaway mechanism on Cu nanotips that can provide this minimum evaporation rate. Moreover, from the perspective of experimental studies, a vacuum breakdown is triggered by a strong local electric field, reaching about 10^{10} V/m [10], which could cause deformation on the surface [20, 21], an intensive field emission [22], and heating of the tip due to Joule [23, 24] and Nottingham effects [25]. As a consequence, a local dense plasma forms at the cathode, radiating light[26-29] and leaving craters on the surface[30-32].

Later on, after the cathodic glow has appeared, light emission is usually observed close to the anode surface as well[1, 28, 33-35], which expands gradually towards the cathode. Many researchers considered the appearance and expansion of anodic glow as a necessary condition for formation of a conductive channel or the transition to the vacuum arc stage, because they observed that the voltage collapses at the moment when the expanding anodic glow reached the cathodic one[33, 34]. Slade *et al.*[1] also expected that the anodic glow would play a major role already before a fully developed vacuum arc carries the full circuit current through a longer gap. In order to elucidate the formation mechanisms of conductive channels in vacuum breakdowns, in a recent work[35], we observed the evolution of the breakdown process by using a high speed ICCD camera with nanosecond resolution. By combining the light emission images with theoretical calculations, we found that the expansion of the anodic glow has no crucial effect on the formation of the conductive path, since the gap voltage drops to a low level much before the anodic glow bridges the gap. Although our observations indicated that the anodic glow is a secondary phenomenon, understanding its nature in detail can be of a valuable assistance in revealing the mechanisms behind the formation of the conductive path and the whole evolution of

the vacuum breakdown. In Ref.[35], we made a first attempt to explain the nature of the anodic glow by hypothesizing that the anode is heated and vaporized due to intense electron bombardment. However, further investigation is required to confirm or refute it. Therefore, we shall here focus on the study of the nature of the anodic glow in detail.

To this end, we conducted a spectroscopic analysis of the glow during the breakdown process, especially near the anode. We used several different materials for the electrodes, including pure copper, brass (alloy of copper and zinc), aluminum and tungsten. We used an Andor spectrometer (SR-500i) with an ICCD camera (Andor DH334T-18U-04) as the spectral detector. We ran our experiments on a tip-to-plane electrode configuration, with gaps of two different lengths, 2 mm and 4 mm. We used an impulse voltage source which provides sufficient power to cause a breakdown through the gap and an output a peak current of 80 A. After the discharge experiments, we examined the electrode

surfaces by SEM (Scanning Electron Microscopy) and EDS (Energy-Dispersive X-ray Spectroscopy) to study their morphology and composition.

2. Experimental setup

2.1. General description

Figure 1 is a schematic diagram of the experimental setup. Electrical discharges occurred in a demountable stainless-steel chamber, which was pumped to a pressure of 2.5×10^{-4} Pa by a turbo molecular pump. A pair of electrodes were installed in the chamber with a variable gap length adjusted by a micrometer manipulator mounted on the lower end of the chamber. The upper and lower electrodes were connected to the high voltage and ground terminals of an impulse voltage source, respectively. The impulse voltage source was set to output a maximum voltage of -40 kV, which maintained a stable arc current of 80 A after the gap breaks down. The pulse duration of the source was uniformly set to 5 μs in all the experiments.
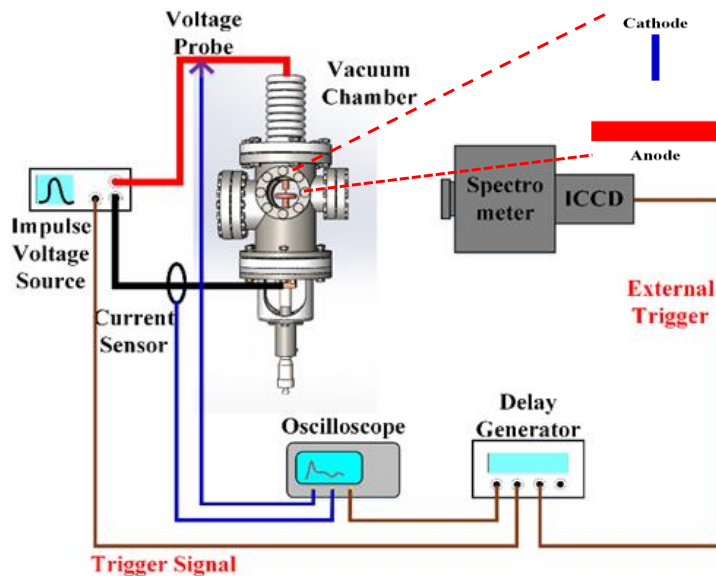

Figure 1. Schematic diagram of the experimental setup. The inset shows the tip-to-plane configuration of electrodes.

The spectrometer and camera were mounted on a 3D movable optical table to collect the

light emission from the vacuum gap through a glass window on the vacuum chamber. An adjustable lens was used together with the movable optical table to ensure that a clear image of the vacuum gap falls on the entrance slit of the spectrometer. The spectrometer has a focal length of 500 mm and a resolution of 0.05 nm with the width of the entrance slit being 10 μm. The spectra were captured by an ICCD camera mounted on the exit flange of the spectrometer. A high voltage probe (NorthStar PVM-7) was used to measure the voltage of the electrode gap. The highest usable voltage and bandwidth are 100 kV and 110 MHz, respectively. The current flowing through the circuit was measured by a Pearson current sensor (Model 6595), which is very suitable for the fast-increasing current during a vacuum discharge because of its bandwidth of 200 MHz. The voltage and current signals were recorded by a four-channel oscilloscope. Finally, a digital delay generator (SRS DG645) acted as a master control to trigger the impulse voltage source, the ICCD camera and the oscilloscope at appropriate time points.

Post-mortem examination of the electrodes was performed by a scanning electron microscope with an energy dispersive X-ray spectrometer (SEM/EDS) manufactured by Hitachi (Model S-3000N), for structural and elemental composition analysis of the electrode surfaces.

2.2. Electrode configuration

In our experiments, we used a tip-to-plane electrode configuration as shown in the inset of Figure 1. We set the upper electrode to be a cathode, since the voltage source supplied a voltage of high negative value. To track the origin of the material found in the flare or on the anode surface, we used different materials for both electrodes, intentionally

selecting metals with different properties. We used cathodes made of tungsten, brass (alloy of copper and zinc) and aluminum, while the anode material was either pure copper or aluminum. The gap length for the tip-to-plane configuration was either 2 mm or 4 mm.

3. Experimental procedure and results

In these experiments, the maximum voltage output of the voltage source was set to -40 kV with a pulse width of 5 μs. The corresponding stable arc current during a breakdown process was 80 A, which was determined by a current-limiting resistance of 500 Ω. The current and voltage waveforms were similar to that in our previous paper[35], because the experimental conditions are similar. The method for recognition of the breakdown instant and determination of the time delay between the recording time and the breakdown instant are also the same as in Ref.[35].

3.1. Overall spectrograms for vacuum breakdowns

Firstly, we examined the spectrum of the light emitted from vacuum breakdowns without any spatial resolution, in the wavelength range between 300 nm and 600 nm. Two different electrode combinations were tested. One was brass-cathode-to-aluminum-anode (BR-Al) and the other aluminum-cathode-to-copper-anode (Al-Cu). Henceforth we shall use this naming convention (cathode material-anode material). A gap length of 4 mm was used in both experiments.

The spectrum analysis for these two cases is shown in Figure 2, where the main spectral peaks are marked with corresponding atom

symbols. We can see that the spectral distributions are quite different between these two cases, except for two common Cu I (324.8 nm and 327.4 nm) peaks, corresponding to deexcitations from copper neutral atoms. For the BR-Al case, we see peaks only from the cathode material in the wavelength range of Figure 2 and no obvious peaks indicating the presence of aluminum, despite the anode being made of aluminum. Most of the peaks correspond to Zn; yet, some weak spectrum peaks corresponding to Cu ions are found as well. On the other hand, for the Al-Cu case, peaks from both cathode and anode materials are present. Many of them correspond to single- (Al II) and double- (Al III) charged aluminum ions.

The intriguing observation in Figure 2 is the absence of aluminum peaks (even the Al I lines, 394.4 nm and 396.1 nm) in the BR-Al case. According to our earlier experiments[35], clear light emission exists near the anode surface in all gaps ranging from 0.5 mm to 30 mm, and the way in which the anodic light expands seemingly indicates that the anode is feeding this anodic glow, so some peaks of the anode material (i.e. Al) were expected to exist.
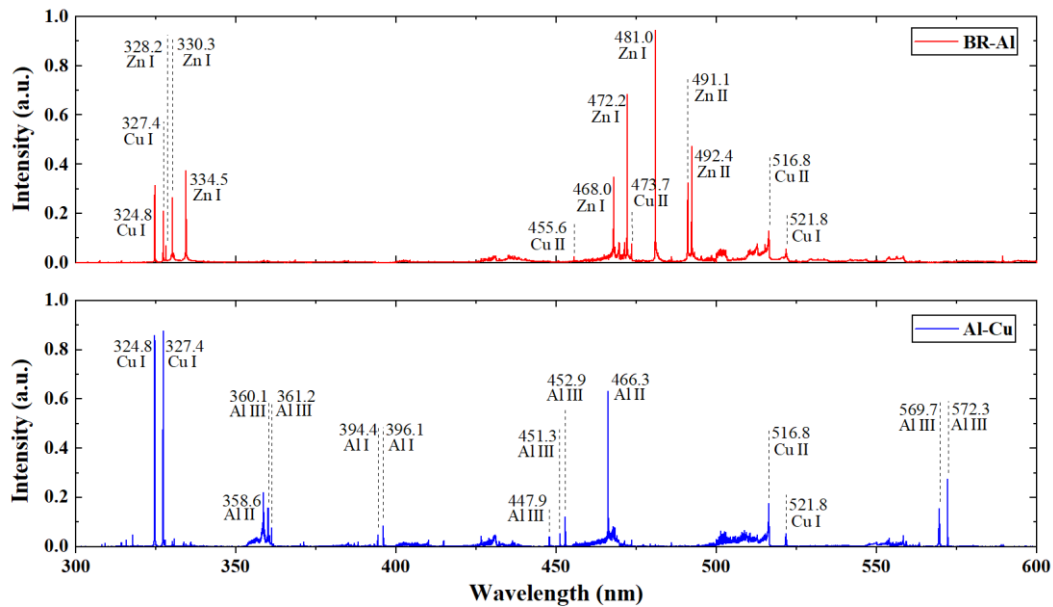

Figure 2. Spectrum distributions for two different electrode combinations. The upper graph is for brass cathode and aluminum anode, while the lower graph is for aluminum cathode and copper anode. Gap length: 4 mm.

To explain this result in the BR-Al case, we further analyze the spatially resolved spectrum distribution of the breakdown glow. The entrance slit of the spectrometer was aligned with the central axis of the vacuum gap. The main peaks in the upper graph of Figure 2 were respectively observed at a time slot of 300 – 500 ns after a breakdown initiation. All the major peaks for the BR-Al case have similar distribution along the gap. The spatial distribution of the two Zn I (neutral zinc atoms) lines (468.0 nm and 472.2 nm) are shown in Figure 3 as an example. Since the intensities of the peaks were too weak to be observed clearly in only one shot of vacuum breakdown, we accumulated 50 shots to obtain a well-pronounced spectrogram as shown in Figure

3. The vertical positions of the cathode tip and the anode surface are indicated by the dashed lines. The Zn I lines at the anode side are easily recognized, since they have a similar spatial distribution as the overall light emission observed in our previous experiments[35]. However, the cathode side is dominated by continuous radiation, which indicates the high temperature and high density of light-emitting ions and atoms there.

We then set the wavelength of the spectrometer to the range of Al I (394.4 nm and 396.1 nm) and confirmed the absence of such lines in the BR-Al case. Based on these spatially resolved spectra, we see that the majority of the anodic light emission is produced by the cathode material, i.e. by copper and zinc in the BR-Al case. In the Al-Cu case, however, we observed both cathode material peaks (Al I, 394.4 nm and 396.1 nm) and anode material peaks (Cu I, 324.8 nm and 327.4 nm) in the anodic glow. This result is better in line with the intuitive expectation of strong dynamics on the anode surface leading to the evaporation of material.

The presence of the cathode material peaks in the spectrum of the anodic glow, along with the absence of aluminum peaks in Figure 2, lead to the following questions:
1) Where do the atoms, which are producing the anodic glow, come from?
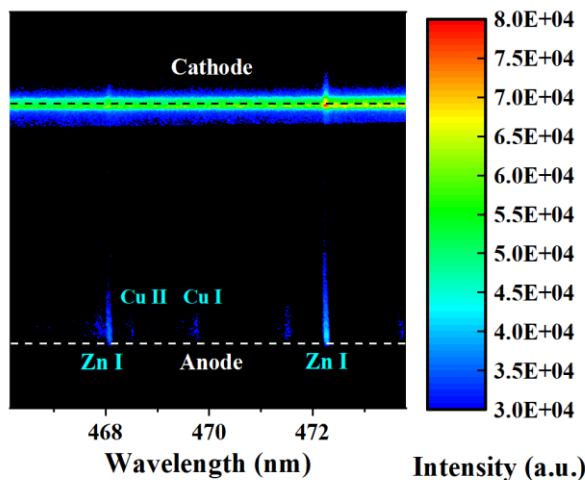2) Why are the Al I lines absent in the BR-Al electrode configuration?

Figure 3. Spatial distribution of Zn spectra in the BR-Al electrode combination. Zn I: 468.0 nm, 472.2 nm. Vertical positions for the cathode and anode are indicated by dash lines.

During the vacuum breakdown process, the atoms in the anodic glow region have two possible sources, the anode and the cathode. The straightforward hypothesis is to assume that the glow near the anode is produced by atoms evaporated from the anode surface, because the glow appears in its immediate vicinity and expands toward the cathode. The alternative hypothesis, i.e. that the anode glow is caused by cathodic atoms is quite counterintuitive, due to the dark region in the middle of the gap. If the atoms in the anodic glow came from the cathode, one would expect that the light emission would be continuously expanding from the cathode to the anode, gradually covering the whole gap, since the atomic density and, hence, the possibility to radiate would be higher in the middle as compared to the anode. However, this is not the case, since the middle of the

gap remains dark[35].

We see nonetheless the cathode material peaks dominating the anodic glow spectrum in the BR-Al case (see Figure 3). This however does not yet prove that the corresponding atoms come from the cathode, since the anode surface might be contaminated by cathode material deposited during previous breakdowns ran with the same electrodes. In order to elucidate this, in the next section we study the anode surface contamination.

3.2. Investigation of material transfer and anode contamination

In this section, we describe experiments analyzing the anode surface contamination. These experiments were conducted in four groups as listed in Table 1. We focused on four peaks in the anodic glow described in Figure 2 and Figure 3. The recording of spectra in group 1 started after the BR-Al electrode system had discharged for hundreds of times, which is the same as the conditions for the recordings of Figure 2 and Figure 3. In other words, assuming an anode contamination process, the anode surface would have been already highly contaminated before the spectrum recording has started. In group 2, we replaced the brass cathode with a tungsten tip, in order to prevent further possible deposition of brass on the aluminum anode and to examine whether a contamination layer of brass still exists on the surface of the aluminum anode. In group 3, a new clean aluminum anode was installed against a new tungsten tip cathode to compare with the experiments of group 2. In group 4, a new aluminum anode and a new brass cathode were used, and the intensity evolution of the observed spectra was recorded as the number of accumulated discharges increases.

Table 1. Experiment groups for evaluating material transfer between electrodes and anode contamination.

Group No.	Gap length (mm)	Cathode material	Anode material	Anode state
1	2	Brass	Aluminum	After discharges with brass cathode
2	2	Tungsten	Aluminum	After used in Group 1
3	2	Tungsten	Aluminum	New
4	4	Brass	Aluminum	New

Figure 4 shows the spectra of the light emission near anode surface under different experimental conditions as described in Table 1. All the images were taken 600 ns after a vacuum breakdown was triggered with an exposure time of 50 ns. The intensities of the spectra were accumulated over 25 shots for each case. The group number corresponding to each image is shown in red color above. In Figure 4(a), the frames labelled as Group 4-1, 4-2 and 4-3 belong to the experiments of group 4, recorded during the shots 51-75, 76-100, and after hundreds of shots for the new aluminum anode correspondingly. In Figure 4(b), the frames labelled as Group 4-1, 4-2 and 4-3 also belong to the group 4, and were recorded during the shots 1-25, 101-125, and after hundreds of shots for the new aluminum anode.

By observing the images in Figure 4, we can see that four Zn I and Zn II peaks are present in group 1, which is similar to Figure 3. Then, in group 2, we also see the same four peaks for Zn I and Zn II, even though the brass cathode has already been replaced by a tungsten one. Since there is no zinc present in the tungsten cathode, the zinc peaks can only be produced by the atoms that came from the anode side. This means that there indeed existed a significant contamination layer of the former cathode material (brass) on the aluminum anode surface. This contamination effect was also confirmed by the results of group 3, in which the four zinc peaks disappeared as expected. From the results of the experiments of group 4 in the last three images of Figure 4(a) and (b), we can see that the intensities of the peaks increase as the breakdown experiments continued, and finally became similar to those of group 1.
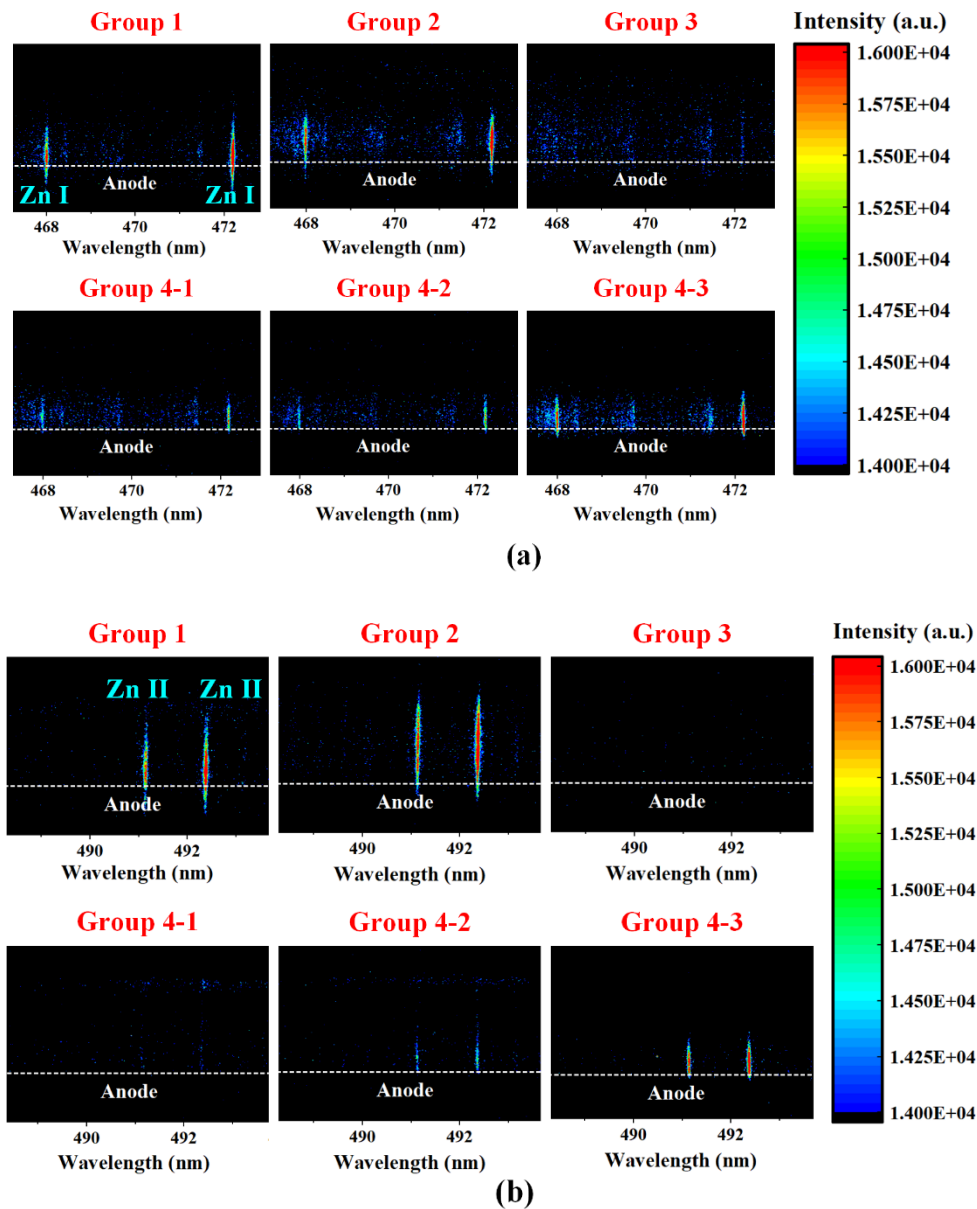

Figure 4. Spectra of the light emission near anode surface under different experimental conditions as

described in Table 1. Frames labelled with Group 4-1, 4-2 and 4-3 in (a) were recorded during shots 51-75, 76-100, and after hundreds of shots. Frames labelled with Group 4-1, 4-2 and 4-3 in (b) were recorded during shots 1-25, 101-125, and after hundreds of shots. Time of exposure: 600-650 ns. Accumulation: 25 shots.

After the vacuum discharge experiments finished, some of the electrodes were taken out of the chamber and examined by a scanning electron microscope (SEM) which is equipped with an EDS analyzer to investigate the elemental composition of the anode surfaces. The results are shown in Figure 5, which consists of six subplots. The gap lengths were 2 mm for the breakdowns between electrodes. The abscissa of each figure represents the X-ray transition energy, while the ordinate represents the intensity of each energy spectrum. There is a SEM picture inset in each EDS figure, which shows the microscopic surface condition and the point of the EDS analysis (indicated by a red circle in the SEM picture). From Figure 5, we can see that many small particles of diameters of several microns appeared on the anode surface after breakdown experiments. According to the EDS results, these small spherical particles come from the cathode, which proves the contamination of the anode surface by cathode materials. We also analyzed the elemental composition of smoother areas on the anode surfaces, see Figure 5(f), where we detected the atoms of the cathode and anode materials as well. These SEM and EDS analyses indicate that the cathode material is deposited on the anode surface in both forms of micron-size particles and condensed vapor.
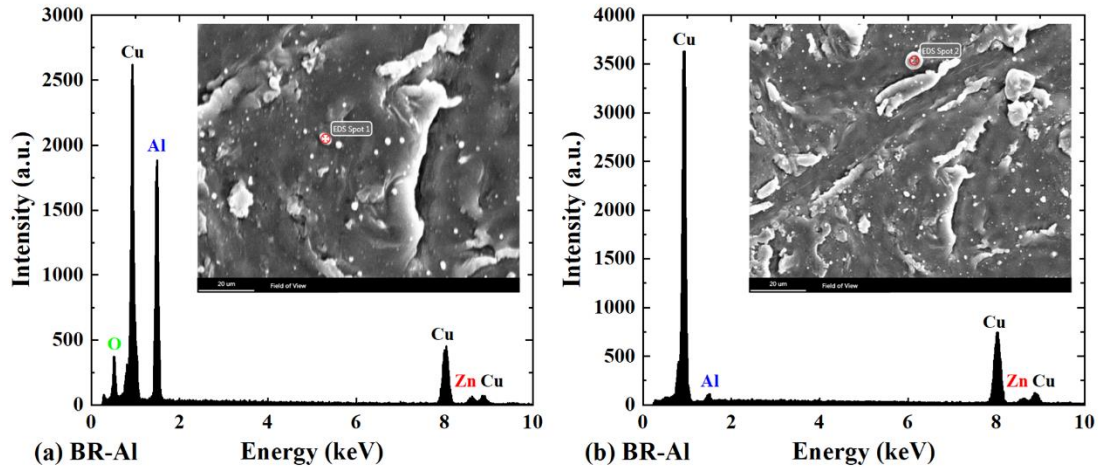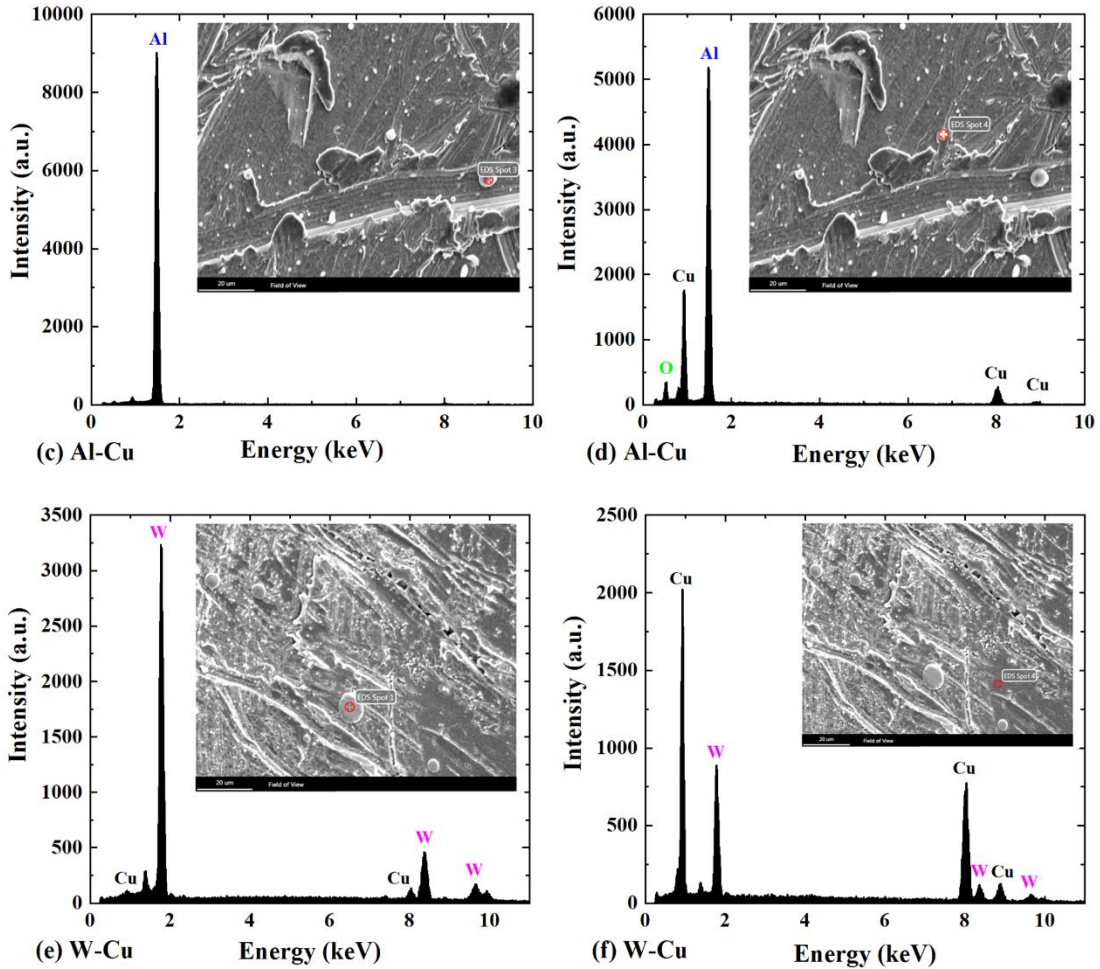
Figure 5. SEM and EDS results for the anode surfaces after vacuum breakdown experiments. (a)-(b): brass cathode to aluminum anode; (c)-(d): aluminum cathode to copper anode; (e)-(f): tungsten cathode to copper anode. Gap length: 2 mm.

Based on the spectroscopic and microscopic analyses described in this section, we conclude that cathode material deposits on the anode surface during a vacuum breakdown, gradually forming a contamination layer. The latter supplies atoms to the anodic glow during the following discharges. Thus, we were able to partially answer the first question in section 3.1. Atoms from the anode surface significantly contribute to the anodic glow.

3.3. Spectra in a clean electrode system

The results presented in the section 1.1 clearly show that atoms coming from the anode contribute in the anodic glow. Yet, it is not clear whether the cathode has a significant contribution. We here aim to elucidate whether the atoms in the anodic glow indeed come only from the anode surface, or the burning cathode flare in the same discharge process contributes to the anodic glow as well.

Although the former is plausible to assume, it is impossible to show it unambiguously as long as the contamination layer exists. Therefore, we tried to observe the spectra of the cathode and anode material in the first few breakdowns right after installation of clean electrodes, in order to exclude the

effects of the anode contamination layer. We also recorded the spectra at the initiation stage of the anodic glow, which appears at about 200 ns for a gap of 4 mm according to our previous results[35], to minimize the effect of the anode contamination during a breakdown.

Figure 6 shows the spectrum distribution of the cathode and anode material for newly installed electrodes. In this, we used two different electrode combinations, brass-cathode-aluminum-anode (BR-Al) and aluminum-cathode-copper-anode (Al-Cu). The results for the BR-Al case are shown in Figure 6(a) and (b), while those of the Al-Cu case are shown in Figure 6(c) and (d). The vertical positions of the electrodes are marked by the dashed lines, and the corresponding atoms for the peaks are shown nearby in blue. We focused our attention on the spectra of the cathode material in the first discharge for each clean electrode combination as shown in Figure 6(a) and (d). The snapshots were taken at 250-350 ns.

We see that there are clear peaks corresponding to the cathode materials (i.e. Cu I in BR-Al case and Al I in Al-Cu case) in the vicinity of the anode surface even at the very early stages of the anodic glow with clean electrodes. This result implies that the cathode flare does provide atoms to the anodic glow region, since the level of anode surface contamination is still too low for a measurable light emission from the atoms evaporated from the contamination layer on the anode surface.

Inspecting carefully the spectrum distribution in Figure 6(a) and (d), we see that the intensities of these cathode material spectra have higher values at the cathode and anode than at the middle of the gap. This is consistent with the images of the overall light emission distribution[35], which show intense light emission near the electrodes and no light in the middle of the gap.

Now we turn our attention to Figure 6(b) and Figure 6(c), which show the distribution of anode material spectra in the second discharge of these electrodes. Figure 6(c) was taken in the time interval of 250-350 ns, while Figure 6(b) was taken during 300-500 ns, since the Al I lines were very weak at earlier times. We clearly see the existence of the anode material peaks near the anode surface, which is consistent with the results of the section 1.1 that the anode provides atoms to the anodic glow. However, we should note here that there are peaks for Al I (394.4 nm and 396.1 nm) in the BR-Al case, which is different from the results in Figure 2. Since the results in Figure 2 were obtained after the electrode system discharged hundreds of time, we also continued to apply voltage pulses to the BR-Al system for 600 times and then recorded the Al I peaks again.

Figure 7 shows the spectroscopic distribution in the wavelength range covering two Al I lines (i.e. 394.4 nm and 396.1 nm). This figure was obtained by accumulating the light intensity over 50 breakdowns from the shots between 601 and 650 to capture any possible existing Al I signals. However, as is shown in Figure 7, we can barely see any signal at the wavelengths related to Al I, which turns out to be consistent with the result in Figure 2. This means that, in the BR-Al case, the aluminum anode gradually stops providing Al atoms for the anodic glow as the number of breakdowns increases. This may be caused by the growing thickness of the contamination layer of the cathode material on the anode surface.
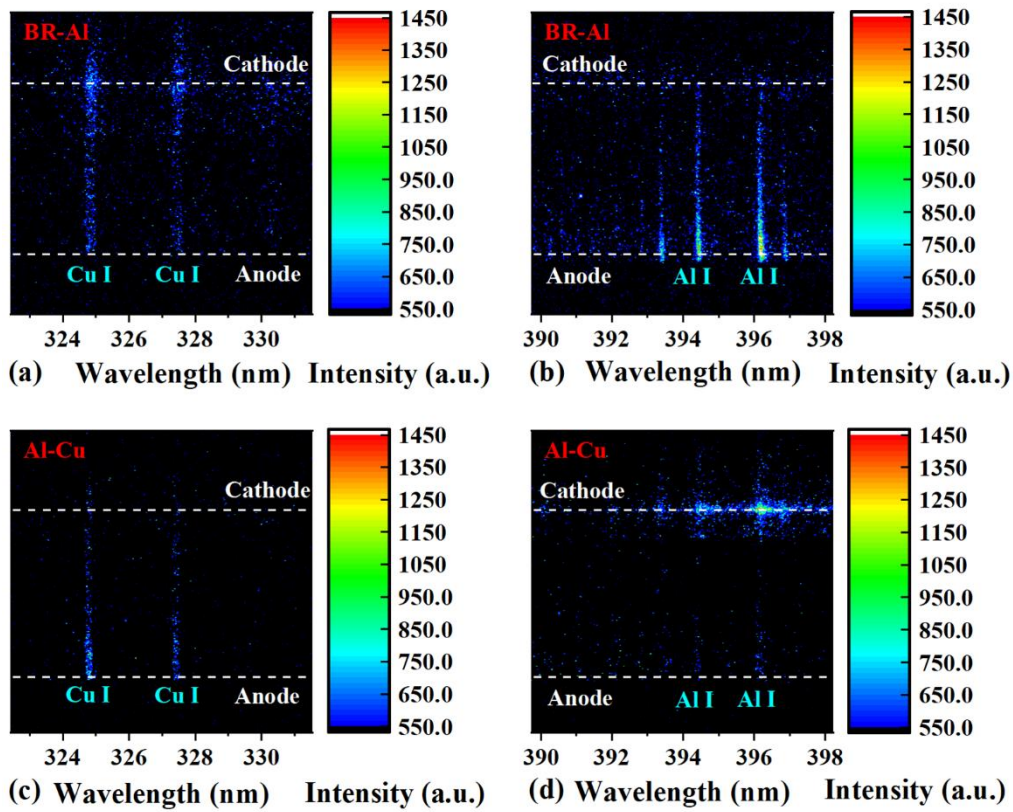
Figure 6. Spectra distribution of cathode and anode material for newly installed electrodes. (a) the first shot of breakdown in a brass-cathode-aluminum-anode system, exposure time from 250–350 ns; (b) the second shot of breakdown in a brass-cathode-aluminum-anode system, exposure time from 300–500 ns; (c) the second shot of breakdown in an aluminum-cathode-copper-anode system, exposure time from 250–350 ns; (d) the first shot of breakdown in an aluminum-cathode-copper-anode system, exposure time from 250–350 ns.
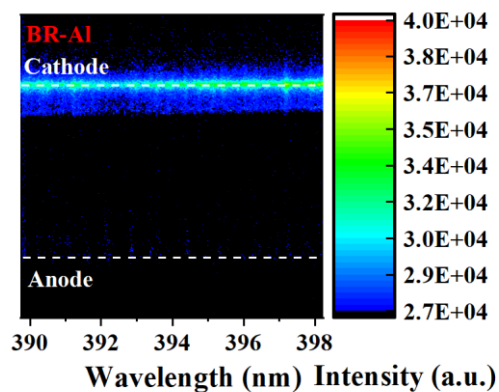

Figure 7. Spectroscopic result of the wavelength range covering Al I (394.4 nm and 396.1 nm). Recording accumulated over breakdown shots 601-650.

3.4. "Covering effect" of contamination layer on the anode surface

In this section, we shall investigate the depth of the anode surface layer that contributes atoms to anodic glow. With this purpose, we designed the experiments that are summarized in Table 2. We prepared three plane anodes for the three groups of experiments with different surface contamination levels. The copper anodes in groups 1 and 3 were subjected to vacuum breakdowns against an aluminum cathode, so there was a contamination layer of aluminum on the copper anode before the experiments began. The aluminum anode in the group 2 was contaminated by materials from the brass cathode, which means that both copper and zinc were present on the surface of the aluminum anode before experiments were conducted.

We focused on the intensities of Cu I and Al I spectra in these experiments plotting the total intensity for each spectral line in Figure 8. The total intensities in Figure 8 were obtained by accumulating the intensities of all pixels in the anodic glow region on the corresponding spectral line, vertically in spectrograms like that in Figure 4. The exposure times for all the spectrograms used in the calculation were set to 7 μs to cover the whole breakdown process, and the intensities were accumulated over 25 discharges for each image. The gap lengths were all 2 mm. The results denoted as Group 3-1, Group 3-2 and Group 3-3 were recorded over the shots 1-25, 276-300 and 526-550, respectively.

Comparing the intensities of Cu I and Al I lines in groups 1 and 2 of Figure 8, we can see that the Cu I spectra were more intense in group 2 (aluminum anode with copper contamination layer), while the Al I spectra were more intense in the group 1 (copper anode with aluminum contamination layer). This means that the contamination layer on the anode surface contributed more than the bulk anode material.

The evolution of the intensities of the two aluminum peaks with more after more discharges can be seen in the group series 3-1, 3-2 and 3-3 in Figure 8. We see that the two aluminum peaks gradually decrease and almost disappear in group 3-3, after over 500 vacuum breakdowns were triggered in the system. This decay of the Al I lines with increasing number of breakdowns indicates that the new contamination of the anode with Cu and Zn reduces the contribution of the previous contamination with Al.

This is also consistent with the top graph of Figure 2, where the Al (anode) spectra are absent. This spectrogram is made after several hundreds of discharges using the same electrodes, thus it is expected that a significant contamination layer has already formed in the anode. This brass layer coats the Al electrode with sufficient coverage to cause the elimination of the Al spectra from the anode glow. However, in the Al-Cu case at the bottom graph of Figure 2, the anode material spectra are not completely absent, although the spectrogram was taken after several hundreds of discharges as well. This implies that in the Al-Cu case the Al contamination on the Cu anode has less coverage, which could be explained by the significantly lower melting point of Al, which causes it to melt and form droplets on the surface, like the one seen in the SEM image of Figure 5(c), instead of a thin coating layer. A more systematic and quantitative study of the formation of the contamination layer and the decay of spectra for anode bulk materials shall be given in a forthcoming

publication.

Table 2. Experiment groups for analyzing the effects of anode contamination layer.

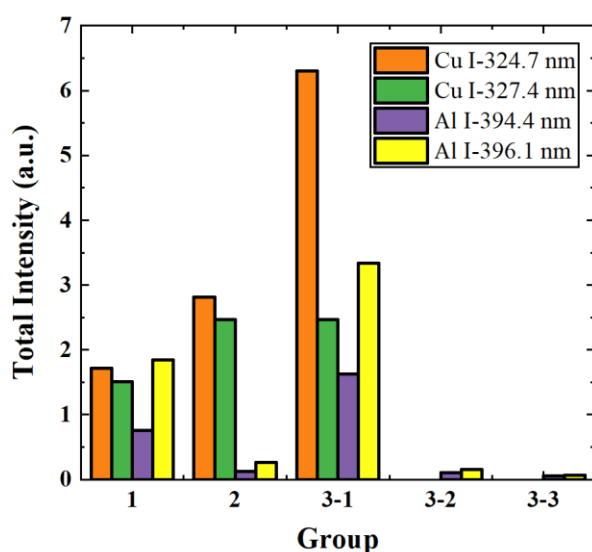| Group No.	Gap length (mm)	Cathode material	Anode material	Anode state
1	2	Tungsten	Copper	After discharges with aluminum cathode
2	2	Tungsten	Aluminum	After discharges with brass cathode
3	2	Brass	Copper	After discharges with aluminum cathode

Figure 8. Total intensities of Cu I and Al I spectra. Exposure time: 7 μs; gap length: 2 mm.

4. Discussion

Our results clearly show that the anodic glow consists of deexcitations from atomic species (both neutrals and ions) originating from both the anode and the cathode electrodes. The undoubtful presence of cathodic species in the anode flare refutes the first "straightforward" hypothesis discussed in section 3.1 and adopted in our previous work[35]. Although the gap remains dark before the appearance of the anode flare, significant amount of cathodic neutrals and ions have reached the anode and contribute to its glow when the latter starts.

This result is consistent with the plasma expansion scenario proposed by Ni and Anders[36]. According to the latter, the dense cathodic plasma expands towards the anode at a supersonic velocity. In our experiments with Cu electrodes, this velocity is estimated by the anode glow delay to be of the order of 10^4 m/s, which is consistent with PIC simulations by Shmelev and Barengolts[37]. For yet unknown reasons, this fast expansion is dark, i.e. the expanding plasma does not emit any detectable light, although high currents run through it. However, when the plasma expansion front reaches the anode electrode, it strongly interacts with the anode material, causing reflection and sputtering of

anodic atoms that are introduced in the plasma and starting emitting light with quite high intensity.

Nevertheless, the exact processes occurring when the cathode atom flux expands and reaches the anode, resulting in an increase of the previously low light emission probability, are still not well understood. The exact mechanisms that cause the dark plasma expansion, the introduction of anodic atoms in the anode flare and the fast expansion of the latter towards the cathode, require further experimental and theoretical investigation.

5. Summary

We conducted spectroscopic and microscopic experiments on the vacuum breakdown processes. The main conclusions can be summarized as follows.

1) Both the cathode and the anode electrodes significantly contribute atoms to the anodic glow. The atoms from the cathode flare reach the anode surface already at the beginning of the anodic glow. The absence of light in the middle of the gap implies the existence of a concentration process for the cathode atoms to start emitting light only in vicinity of the anode. Further investigation of the nature of this process is required.

2) The cathode material contaminates the anode surface during the process of vacuum breakdown, resulting in a layer of cathode material on the anode surface. This contamination layer includes both smoothly condensing cathode vapor and micron-sized spherical particles.

3) Only a thin layer of the anode surface contributes to the anodic glow, as shown by the fact that the gradually increasing contamination layer on the anode surface

causes the decay and possible elimination of the anode bulk signals in the anode glow spectra.

Reference

[1]   Slade P G 2007 *The vacuum interrupter: theory, design, and application*: CRC press)

[2]   Clements J S, Sato M and Davis R H 1987 Preliminary investigation of prebreakdown phenomena and chemical reactions using a pulsed high-voltage discharge in water *IEEE Transactions on Industry Applications* 224-35

[3]   Park J, Henins I, Herrmann H and Selwyn G 2001 Gas breakdown in an atmospheric pressure radio-frequency capacitive plasma source *journal of Applied Physics* **89** 15-9

[4]   Wiesmann H and Zeller H 1986 A fractal model of dielectric breakdown and prebreakdown in solid dielectrics *Journal of applied physics* **60** 1770-3

[5]   Jüttner B 2001 Cathode spots of electric arcs *Journal of Physics D: Applied Physics* **34** R103

[6]   McCracken G 1980 A review of the experimental evidence for arcing and sputtering in tokamaks *Journal of*

Nuclear Materials **93** 3-16

[7]   De Lara J, Pérez F, Alfonseca M, Galán L, Montero I, Román E and Garcia-Baquero D R 2006 Multipactor prediction for on-board spacecraft RF equipment with the MEST software tool *IEEE Transactions on Plasma Science* **34** 476-84

[8]   Rozario N, Lenzing H F, Reardon K F, Zarro M S and Baran C G 1994 Investigation of Telstar 4 spacecraft Ku-band and C-band antenna components for multipactor breakdown *IEEE transactions on microwave theory and techniques* **42** 558-64

[9]   Dobert S, Adolphsen C, Bowden G, Burke D, Chan J, Dolgashev V, Frisch J, Jobe K, Jones R and Lewandowski J 2005 High gradient performance of NLC/GLC X-band accelerating structures. In: *Particle Accelerator Conference, 2005. PAC 2005. Proceedings of the*: IEEE) pp 372-4

[10]   Descoeudres A, Levinsen Y, Calatroni S, Taborelli M and Wuensch W 2009 Investigation of the dc vacuum breakdown mechanism *Physical Review Special Topics-Accelerators and Beams* **12** 092001

[11]   Aicheler M, Burrows P, Draper M, Garvey T, Lebrun P, Peach K, Phinney N, Schmickler H, Schulte D and Toge N 2014 A Multi-TeV linear collider based on CLIC technology: CLIC Conceptual Design Report. SLAC National Accelerator Lab., Menlo Park, CA (United States))

[12]   Lyon D and Hubler A 2013 Gap size dependence of the dielectric strength in nano vacuum gaps *IEEE Transactions on Dielectrics and Electrical Insulation* **20** 1467-71

[13]   Ducharme S 2009 An inside-out approach to storing electrostatic energy *ACS nano* **3** 2447-50

[14]   Sterling R, Hughes M, Mellor C and Hensinger W 2013 Increased surface flashover voltage in microfabricated devices *Applied Physics Letters* **103** 143504

[15]   Mesyats G A 2013 Ecton mechanism of the cathode spot phenomena in a vacuum arc *IEEE Transactions on Plasma Science* **41** 676-94

[16]   Mesyats G A 1995 Ecton or electron avalanche from metal *Physics-Uspekhi* **38** 567-90

[17]   Timko H, Matyash K, Schneider R, Djurabekova F, Nordlund K, Hansen A, Descoeudres A, Kovermann J, Grudiev A, Wuensch W, Calatroni S and Taborelli M 2011 A One-Dimensional Particle-in-Cell Model of Plasma Build-Up in Vacuum Arcs *Contributions to Plasma Physics* **51** 5-21

[18]   Timko H, Ness Sjobak K, Mether L, Calatroni S, Djurabekova F, Matyash K, Nordlund K, Schneider R and Wuensch W 2015 From Field Emission to Vacuum Arc Ignition: A New Tool for Simulating Copper Vacuum Arcs *Contributions to Plasma Physics* **55** 299-314

[19]   Kyritsakis A, Veske M, Eimre K, Zadin V and Djurabekova F 2018 Thermal runaway of metal nano-tips during intense electron emission *Journal of Physics D: Applied Physics* **51** 225203

[20]   Yanagisawa H, Zadin V, Kunze K, Hafner C, Aabloo A, Kim D E, Kling M F, Djurabekova F, Osterwalder J and Wuensch W 2016 Laser-induced

asymmetric faceting and growth of a nano-protrusion on a tungsten tip *APL Photonics* **1** 091305

[21] Fujita S and Shimoyama H 2007 Mechanism of surface-tension reduction by electric-field application: Shape changes in single-crystal field emitters under thermal-field treatment *Physical Review B* **75** 235431

[22] Fursey G 2003 Field emission in vacuum micro-electronics *Appl Surf Sci* **215** 113-34

[23] Dyke W P and Trolan J K 1953 Field Emission - Large Current Densities, Space Charge, and the Vacuum Arc *Phys Rev* **89** 799-808

[24] Dyke W P, Trolan J K, Martin E E and Barbour J P 1953 The Field Emission Initiated Vacuum Arc .I. Experiments on Arc Initiation *Phys Rev* **91** 1043-54

[25] Charbonnier F, Strayer R, Swanson L and Martin E 1964 Nottingham effect in field and t− f emission: Heating and cooling domains, and inversion temperature *Physical Review Letters* **13** 397

[26] Mazurek B and Cross J D 1988 Fast cathode processes in vacuum discharge development *Journal of Applied Physics* **63** 4899-904

[27] Mazurek B, Nowak A and Tyman A 1993 X-ray emission accompanying cathode microdischarge *Ieee T Electr Insul* **28** 488-93

[28] Inada Y, Kamiya T, Matsuoka S, Kumada A, Ikeda H and Hidaka K 2018 Two-dimensional electron density visualization over plasma flare in vacuum breakdown process *J Appl Phys* **124** 083301

[29] Zhao L, Su J-c, Zhang X-b, Li R, Zheng L, Zeng B, Cheng J, She X-y and Wu X-l 2015 A large-dynamic-range current probe for microsecond pulsed vacuum breakdown research *Rev Sci Instrum* **86** 015109

[30] Shipman N C 2014 Experimental study of DC vacuum breakdown and application to high-gradient accelerating structures for CLIC. The University of Manchester)

[31] Djurabekova F, Samela J, Timko H, Nordlund K, Calatroni S, Taborelli M and Wuensch W 2012 Crater formation by single ions, cluster ions and ion "showers" *Nuclear Instruments and Methods in Physics Research Section B: Beam Interactions with Materials and Atoms* **272** 374-6

[32] Timko H, Djurabekova F, Nordlund K, Costelle L, Matyash K, Schneider R, Toerklep A, Arnau-Izquierdo G, Descoeudres A and Calatroni S 2010 Mechanism of surface modification in the plasma-surface interaction in electrical arcs *Physical Review B* **81** 184109

[33] Mesyats G 2000 Cathode Phenomena in a Vacuum Discharge: The breakdown, the spark, and the arc. Moscow, Russia: Nauka)

[34] Chalmers I D and Phukan B D 1979 Photographic Observations of Impulse Breakdown in Short Vacuum Gaps *J Phys D Appl Phys* **12** 1285-&

[35] Zhou Z, Kyritsakis A, Wang Z, Li Y, Geng Y and Djurabekova F 2019 Direct observation of vacuum arc evolution with nanosecond resolution *Scientific Reports* **9** 7814

[36] Ni P A and Anders A 2010 Supersonic metal plasma impact on a surface: An optical investigation of the pre-surface region *Journal of*

Physics D: Applied Physics **43** 135201

[37] Shmelev D L and Barengolts S A 2013 Modeling of cathode plasma flare expansion *IEEE Transactions on Plasma Science* **41** 1964-8